JPET Fast Forward. Published on June 9, 2017 as DOI: 10.1124/jpet.117.240309
This article has not been copyedited and formatted. The final version may differ from this version.

1 Title Page

Title:

Semi-mechanistic bone marrow exhaustion pharmacokinetic/pharmacodynamic model for chemotherapy-induced cumulative neutropenia

Authors: Andrea Henrich, Markus Joerger, Stefanie Kraff, Ulrich Jaehde, Wilhelm Huisinga, Charlotte Kloft, Zinnia Patricia Parra-Guillen

Primary laboratory of origin: Dept. Clinical Pharmacy & Biochemistry, Institute of Pharmacy, Freie Universitaet Berlin, Germany

Affiliations (indicated by authors' initials only):

AH, CK, ZP-G: Dept. Clinical Pharmacy & Biochemistry, Institute of Pharmacy, Freie Universitaet Berlin, Germany

AH: Graduate Research Training program PharMetrX, Germany

MJ: Dept. of Oncology & Haematology, Cantonal Hospital, St. Gallen, Switzerland

SK, UJ: Dept. Clinical Pharmacy, Institute of Pharmacy, Universitaet Bonn, Germany

WH: Institute of Mathematics, Universitaet Potsdam, Germany

JPET Fast Forward. Published on June 9, 2017 as DOI: 10.1124/jpet.117.240309
This article has not been copyedited and formatted. The final version may differ from this version.

2 Running title Page

a) Running title

Bone marrow exhaustion PKPD model for cumulative neutropenia

b) Corresponding author:

Charlotte Kloft, Zinnia P. Parra-Guillen

Freie Universitaet Berlin

Institute of Pharmacy

Department of Clinical Pharmacy & Biochemistry

Kelchstr. 31

12169 Berlin/Germany

Phone: +49-30-838 50656

Fax: +49-30-838 450656

Charlotte.kloft@fu-berlin.de

c) The number of

- Text pages: 18
- Tables: 2
- Figures: 4
- References: 41
- Words in the abstract: 239
- Words in the introduction: 696
- Words in the discussion: 1664

JPET Fast Forward. Published on June 9, 2017 as DOI: 10.1124/jpet.117.240309
This article has not been copyedited and formatted. The final version may differ from this version.

d) List of nonstandard abbreviations, in alphabetical order.

AIC	Akaike Information Criterion
AUC	Area under plasma concentration-time curve
$Base_1$	Baseline of proliferating cells not affected by time-dependent depletion
$Base_2$	Baseline of proliferating cells affected by time-dependent depletion
$BASE_{tot}(t)$	Total baseline of proliferating cells at time t in Model A
$BASE_{tot}(t_0)$	Total baseline of proliferating cells at time t=0 in Model A
BILI	Bilirubin concentration
BME	Bone marrow exhaustion
BSA	Body surface area
Central	Central paclitaxel compartment
CEPAC-TDM	CESAR (Central European Society for Anticancer Drug Research) study of Paclitaxel Therapeutic Drug Monitoring
Circ	Circulating neutrophil cell compartment
$Circ_0$	Individually measured baseline neutrophil concentration including residual variability
Circ(t)	Concentration of circulating neutrophils at time t
$Circ(t_0)$	Concentration of circulating neutrophils at time t=0
$C_{PTX}(t)$	Paclitaxel plasma concentration at time t
$C_{Platin}(t)$	Plasma concentration of carbo- or cisplatin at time t, respectively
EBE	Empirical Bayes Estimates (individual PK or PD parameters)
E_{drug}	Drug effect inhibiting k_{prol} in Model A-C and k_{stem} in Model C
E_{drug2}	Additional time-dependent drug effect affecting $Base_2$ in Model A
FB	Feedback
F_{prol}	Fraction of proliferating cells entering maturation chain and not entering quiescent cell cycle in Model B
frB	Fraction of $BASE_{tot}(t_0)$ not affected by depletion in Model A
f_{tr}	Fraction of input in Prol via replication in Model C
k	Number of parameters estimated in a model
k_{21}	Distribution rate constant between Central and Per1
k_{cycle}	Circulation rate constant within quiescent cell cycle

JPET Fast Forward. Published on June 9, 2017 as DOI: 10.1124/jpet.117.240309
This article has not been copyedited and formatted. The final version may differ from this version.

k_{depl}	Depletion rate constant of E_{drug2} in Model A
Km_{EL}	Paclitaxel concentration at half VM_{EL}
Km_{TR}	Paclitaxel concentration at half VM_{TR}
k_{prol}	Proliferation rate constant of cells in Prol
k_{stem}	Proliferation rate constant of cells in Stem
k_{tr}	Transition rate constant of maturation chain
MAP	Maximum a posteriori
$MARPE_p$	Median absolute relative prediction error for parameter p
MMT	Mean maturation time
$MRPE_p$	Median relative prediction error for parameter p
NSCLC	Non-small cell lung cancer
OFV	Objective function value
pcVPC	Prediction-corrected visual predictive check
PD	Pharmacodynamic(s)
Per1	1st peripheral compartment of paclitaxel
Per2	2st peripheral compartment of paclitaxel
$P_{i,o,optimized}$	Parameter of individual i, at occasion o, obtained by optimized PK model
$P_{i,o,original}$	Parameter of individual i, at occasion o, obtained by original PK model
$P_{i,o,re\text{-}est}$	Parameter of individual i, at occasion o, obtained by *post-hoc* re-estimation
$P_{i,o,sim}$	Parameter of individual i, at occasion o, obtained by simulation
PK	Pharmacokinetic(s)
Prol	Proliferating cell compartment
Q	Intercompartmental clearance between Central and Per2
Q1	1st quiescent cell compartment in Model B
Q2	2nd quiescent cell compartment in Model B
$RPE_{p,i,o}$	Relative prediction error of parameter p, for individual i, at occasion o
RSE	Relative standard error
SL	Slope factor of linear drug effect of paclitaxel
SL_{Platin}	Slope factor of linear drug effect of platinum-based drugs
Stem	Stem cell compartment in Model C

JPET Fast Forward. Published on June 9, 2017 as DOI: 10.1124/jpet.117.240309
This article has not been copyedited and formatted. The final version may differ from this version.

t	Time
$T_{C>0.05}$	Time C_{PTX} above 0.05 µmol/L in respective cycle
Transit	Transit compartment of maturation chain (3 for Model A-C)
V_1	Central volume of distribution
V_3	Volume of distribution of Per2
VM_{EL}	Maximum elimination capacity
VM_{TR}	Maximum transport capacity
γ	Exponent of feedback function

e) Section assignment to guide the listing in the table of contents:

Chemotherapy, Antibiotics, and Gene Therapy

JPET Fast Forward. Published on June 9, 2017 as DOI: 10.1124/jpet.117.240309
This article has not been copyedited and formatted. The final version may differ from this version.

3 Abstract

Paclitaxel is a commonly used cytotoxic anticancer drug with potentially life-threatening toxicity at therapeutic doses and high interindividual pharmacokinetic variability. Thus, drug and effect monitoring is indicated to control dose-limiting neutropenia. A dose individualization algorithm was developed by Joerger *et al.* based on a pharmacokinetic/pharmacodynamic (PK/PD) model describing paclitaxel and neutrophil concentrations. Further, the algorithm was prospectively compared in a clinical trial against standard dosing (CEPAC-TDM study, $n_{patients}$=365, n_{cycles}=720) but did not substantially improve neutropenia. This might be caused by misspecifications in the PK/PD model underlying the algorithm, especially without consideration of the observed cumulative pattern of neutropenia or the platinum-based combination therapy, both impacting neutropenia. The aim of this work was to externally evaluate the original PK/PD model for potential misspecifications and to refine together with considering the cumulative neutropenia pattern and the combination therapy. For PK ($n_{samples}$=658), an underprediction was observed and the PK parameters were re-estimated using the original estimates as prior information. Neutrophil concentrations ($n_{samples}$=3274) were overpredicted by the PK/PD model especially for later treatment cycles, when the cumulative pattern aggravated neutropenia. Three different modelling approaches (two from literature, one newly developed) were investigated and the newly developed one, implementing the bone marrow hypothesis semi-physiologically, was superior. This model further included an additive effect for toxicity of the carboplatin combination therapy. Overall, a physiologically plausible PK/PD model was developed that can be used for dose adaptation simulations and prospective studies to further improve paclitaxel-carboplatin-combination therapy.

4 Introduction

Cytotoxic drugs used in cancer treatment typically have a narrow therapeutic window, with severe toxicity caused by their unspecific mode of action affecting rapidly dividing cells on one side, and the need for sufficiently high doses for efficacy on the other side (Gurney, 1996). Paclitaxel is a cytotoxic which is wildly used in different cancer types. It enhances and stabilizes the polymerization of microtubules, leading to clinically relevant toxicity, especially dose-limiting neutropenia. This frequent and severe adverse event is caused by the cytotoxic effect on proliferating cells, particularly bone marrow progenitor cells, leading to potentially life-threatening infections (Mitchison, 2012). Neutropenia caused by paclitaxel-containing combination therapies can even be cumulative, meaning a worsening of neutropenia over the repeated treatment cycles (Huizing, *et al.*, 1997). In addition, the pharmacokinetics (PK) of paclitaxel administered in a formulation with Cremophor EL is nonlinear, schedule-dependent (e.g. influence of infusion duration) and exhibits high interindividual variability. The time of paclitaxel plasma concentration above the threshold of 0.05 µmol/L ($T_{C>0.05}$) was found to be a relevant PK exposure surrogate for toxicity (Gianni *et al.*, 1995; Ohtsu *et al.*, 1995; Huizing, *et al.*, 1997; Lichtman *et al.*, 2006; Joerger *et al.*, 2007) and efficacy (Huizing, *et al.*, 1997; Joerger *et al.*, 2007), i.e. 26-31 h (Joerger *et al.*, 2012). The combination of narrow therapeutic window and high interindividual variability highly favors dose individualization based on therapeutic drug monitoring.

Currently the dose of paclitaxel is adjusted by body surface area (BSA), found to be influential on paclitaxel PK (Smorenburg *et al.*, 2003), but not by other relevant factors such as organ (dys)function or age (Mielke *et al.*, 2007). Furthermore, paclitaxel is typically part of a combination therapy with carbo- or cisplatin displaying toxic effects on the haematopoietic system as well. In summary, individualized therapy of paclitaxel combination therapy is needed to balance toxicity and efficacy.

Pharmacokinetic/pharmacodynamic (PK/PD) modelling and simulation is suggested as a tool to improve the dosing of paclitaxel by reducing toxicity without compromising efficacy given the complex PK of paclitaxel and the combination therapy (Joerger *et al.*, 2016). Based on a pooled PK/PD analysis from several clinical trials including different cancer types, a PK/PD model to characterize paclitaxel plasma concentrations (PK) and resulting neutropenia (PD) was developed (Joerger *et al.*, 2012). The PK was described by a 3 compartment model including nonlinear distribution and elimination, while for the PD the neutropenia model structure developed by Friberg *et al.* (Friberg *et al.*, 2002) was applied for paclitaxel-associated neutropenia. The PK/PD model was then utilized to develop a dose

JPET Fast Forward. Published on June 9, 2017 as DOI: 10.1124/jpet.117.240309
This article has not been copyedited and formatted. The final version may differ from this version.

individualization algorithm, considering different covariates (BSA, age, sex) as well as target drug exposure ($T_{C>0.05}$) and toxicity (grade of neutropenia) from the previous cycle. Next, the dosing algorithm was applied in the CEPAC-TDM trial (CESAR study of paclitaxel therapeutic drug monitoring (Joerger *et al.*, 2016)). The aim of this prospective, multicenter, randomized, controlled clinical study was to investigate whether therapeutic drug monitoring and target-concentration intervention, based on sparse sampling, of paclitaxel was able to reduce toxicity while maintaining efficacy compared to standard BSA-based dosing of paclitaxel. The results showed that the exposure target of the $T_{C>0.05}$ (26-31 h) was not met in more than 50% patients, and no significant improvement of grade 4 neutropenia was achieved for patients in the experimental arm (Joerger *et al.*, 2007). Nevertheless, paclitaxel-related neuropathy was substantially improved. With this clinical trial, an important step towards an optimal and individualized dosing of paclitaxel in combination with cis-/carboplatin was done. Reasons for the lack of improvement of paclitaxel-related neutropenia may include suboptimal PK and PD models used for the paclitaxel dosing algorithm as used in the CEPAC-TDM trial. Thus, further improvement in the models and the dosing algorithm are needed to reduce the toxic burden for the patients.

The aim of the present study was to investigate the appropriateness of the original PK/PD model for the data from the CEPAC-TDM trial and detect potential model misspecifications. Furthermore, the PK/PD model should be optimized to be able to adequately capture cumulative neutropenia after repeated treatment cycles of paclitaxel in combination with cis-/carboplatin. The optimized model shall consider physiological plausibility to be able to simulate different dose optimization scenarios of the paclitaxel combination chemotherapy.

JPET Fast Forward. Published on June 9, 2017 as DOI: 10.1124/jpet.117.240309
This article has not been copyedited and formatted. The final version may differ from this version.

5 Materials and Methods

Clinical data

To evaluate the previously developed PK/PD model, data from the CEPAC-TDM study (Joerger *et al.*, 2016) carried out in accordance with the Declaration of Helsinki and approved by the Institutional Review Boards were use. Briefly, patients with newly diagnosed advanced non-small cell lung cancer (NSCLC) were treated with paclitaxel (3 h intravenous infusion) in combination with either cis- or carboplatin every 3 weeks for up to 6 cycles. 182 patients (740 treatment cycles in total) in the conventional study arm received the standard dose of paclitaxel (200 mg/m²), while 183 patients (720 treatment cycles in total) in the experimental study arm received a paclitaxel dose adapted to sex, age and BSA for the first treatment cycle. In the following cycles, the dose for these patients was further adapted based on i) the experienced grade of neutropenia and ii) the paclitaxel exposure, expressed as $T_{C>0.05}$ both of the previous cycle. PK samples were only taken from patients in the experimental arm, once per cycle (approx. 24 h (16-30 h) after start of infusion), since only here the dose adaptation based on $T_{C>0.05}$ was performed. $T_{C>0.05}$ was determined by *post-hoc* estimation with the original PK model in NONMEM. PD samples (neutrophil measurements) were taken in both arms at baseline, on day 1 and day 15±2 in each cycle and finally at the end of treatment visit. Paclitaxel concentrations were determined by liquid-chromatography and UV detection (lower limit of quantification: 0.015 mg/L (=0.017 µmol/L); recovery: 90.6±9.63; overall precision: <10%) (Zufía López *et al.*, 2006). Neutrophil concentrations were measured in routine clinical chemistry analysis at each study side.

The low number of measurements below the lower limit of quantification (PK: 0.30%, PD: 0.40%) as well as missing samples (PK: 8.61%; PD of conventional arm: 11.4%; of experimental arm: 9.25%) were assumed to be missing completely at random and removed from the subsequent PK/PD analysis. For these, primarily data from the experimental arm were considered, since only these patients underwent paclitaxel PK sampling. Only for evaluation of the newly developed PK/PD model, dosing information, neutrophil concentration measurements and covariate data from the conventional arm were used. A summary of patient characteristics can be found in (Joerger *et al.*, 2016) and a summary of the entire modelling and simulation workflow can be found in the Supplemental Figure 1.

Original PK model and external evaluation

The analysis was based on a previously published PK/PD model ("original model") (Joerger *et al.*, 2012), which was also used to develop the CEPAC TDM dosing algorithm. The PK of paclitaxel was described by a three-compartment model (Figure 1, upper left panel) with nonlinear distribution to the first peripheral compartment and non-linear elimination. BSA, sex, age and total bilirubin concentration (BILI) were implemented as covariates on the maximum elimination capacity (VM_{EL}) using power relations. An exponential model was assumed for interindividual, interoccasion and residual variability.

This PK model was externally evaluated using the data from the experimental arm of the CEPAC-TDM study. For this purpose, *post-hoc* estimation with the original PK model was performed to obtain individual PK parameters (empirical Bayesian estimates, EBE) and the individually predicted paclitaxel concentration-time profiles. Model performance was then evaluated by basic goodness-of-fit plots, shrinkage (Savic and Karlsson, 2009) and comparing 1000 simulations with the study data in prediction-corrected visual predictive checks (pcVPC) (Bergstrand *et al.*, 2011). As in the original model the first-order conditional estimation method with interaction was used for all PK analyses.

PK model optimization using prior information

To refine the PK model for the population in the CEPAC-TDM study, the final PK parameter estimates and their precision (diagonal elements of the variance-covariance matrix), retrieved from the original PK model, were implemented in the maximum a posteriori (MAP) Bayesian approach (originally referred to as frequentist approach) as prior information using the Normal-InverseWishart distribution (Gisleskog *et al.*, 2002). Interoccasion variability was not re-estimated but assumed to be the same as originally estimated, since only one PK measurement per cycle (= occasion) was available. The degrees of freedom for estimating interindividual variability were calculated as described in (Bauer, 2014) while for the residual variability 1000 was chosen as the lowest number allowing stable estimation.

The optimized PK parameters were compared with the original ones at the population and individual level. A bootstrap analysis (Efron and Tibshirani, 1986) (1000 bootstrap datasets) was performed to evaluate parameter precision and the 95% confidence intervals were compared as well as population parameter estimates. Confidence intervals of the original model were calculated based on the standard error, retrieved from the original model, assuming normal distribution. To evaluate improvements of the model prediction, a pcVPC was generated (n=1000 simulations).

Prediction errors between individual parameter estimates, taking the optimized PK model as reference and comparing with the original PK model, were calculated as bias and imprecision according to the following equations (Sheiner and Beal, 1981):

$$RPE_{p,i,o} = \left(P_{i,o,original} - P_{i,o,optimized}\right)/P_{i,o,optimized} \quad (1)$$

$$MRPE_p = median\left(RPE_{p,i,o}\right) \quad (2)$$

$$MARPE_p = median\left(\left|RPE_{p,i,o}\right|\right) \quad (3)$$

in which $P_{i,o,original}$ and $P_{i,o,optimized}$ were the EBEs and exposure parameters ($T_{C>0.05}$ and area under the curve (AUC)) of individual "i" at occasion "o" (if interoccasion variability was applicable) based on the original and the optimized model, respectively; $RPE_{p,i,o}$ was the relative prediction error between the original and the optimized parameter, for each model parameter "p", $MRPE_p$ was the median relative prediction error indicating bias and $MARPE_p$ was the absolute (unsigned) value of the relative prediction error expressing imprecision for each parameter taking as reference the optimized parameters.

Original PK/PD model and external evaluation

The neutrophil concentrations in (Joerger *et al.*, 2012) were described by the semi-mechanistic neutropenia PK/PD model developed by Friberg *et al*. For the sequential PK/PD analysis EBEs of the optimized population PK parameters and the associated individual concentration-time profiles of paclitaxel were used to inform the drug effect (E_{drug}) of the PK/PD model by introducing a linear PK/PD relationship with slope factor (SL). This method implies a cytostatic drug effect if $E_{drug} \leq 1$ and a cytotoxic effect if $E_{drug} > 1$, since the proliferating rate constant k_{prol} was multiplied by $1-E_{drug}$.

In the Friberg *et al.* model the granulopoiesis was described by a chain of 5 compartments, of which the first represents the proliferating cells (Prol). These cells replicate (with the proliferating rate constant k_{prol}) and then mature and differentiate via a chain of n=3 transit compartments with a transition rate constant k_{tr} obtained from the mean maturation time (MMT): k_{tr}=MMT/(number of transitions), until they are circulating neutrophil (Circ) that can be measured in the blood. Finally, the circulating neutrophils can be eliminated by a first-order process. To gain homeostasis of the system, this elimination rate constant was assumed to be equal to k_{prol} and k_{tr}. At the same time, k_{prol} was influenced by E_{drug} in an inhibitory manner and a feedback mechanism (FB) responsible for the recovery after drug administration. An exponential model was assumed for interindividual variability on SL, MMT and for residual variability.

JPET Fast Forward. Published on June 9, 2017 as DOI: 10.1124/jpet.117.240309
This article has not been copyedited and formatted. The final version may differ from this version.

For the external evaluation of this PK/PD model the same steps as for the PK model were performed. As in the original model, the first-order estimation method was used.

PK/PD model optimization

Based on the external evaluation of the PK/PD model and the observed long-term decay in the neutrophil concentrations over the cycles, a pattern of cumulative neutropenia over the repeated treatment cycles was detected. To account for this pattern, PK/PD model extensions of the Friberg *et al.* PK/PD model were investigated: Two published models (Bender *et al.*, 2012; Mangas-Sanjuan *et al.*, 2015) were identified (Model A, Model B, respectively) and a new PK/PD model was developed and evaluated (Model C). A schematic representation of all 3 models including their modifications from the Friberg *et al.* PK/PD model, can be found in Fig 1A-C:

Briefly: **Model A** (Fig 1A) (based on Bender *et al.*, 2012), was originally developed to describe thrombocytopenia in patients treated with trastuzumab emtansine. In this model, the circulating cells (originally thrombocytes, here neutrophils) at baseline ($BASE_{tot}(t_0)$) were assumed to belong to two different subpopulations ($BASE_1$ and $BASE_2$). $BASE_2$ was affected by a second time-dependent drug effect (E_{drug2}), leading to a reduction of the total baseline over time ($BASE_{tot}(t)$), which was the target value of the feedback mechanism. While originally the average concentration of trastuzumab emtansine was determining the extent of this second drug effect E_{drug2}, here $T_{C>0.05}$ of paclitaxel of each cycle was assumed to drive this effect. Additionally to the PD parameters estimated in the original model (MMT, γ, SL), the fraction of $BASE_{tot}(t_0)$ not affected by the second drug effect (frB), as well as the depletion rate constant of E_{drug2} on $BASE_2$ (k_{depl}) were estimated.

Model B (Fig 1B) (based on Mangas-Sanjuan *et al.*, 2015) was originally developed to describe neutropenia after different doses of diflomotecan. Compared to the Friberg *et al.* model, two additional compartments accounting for a cyclic cell pathway from Prol to Prol with two stages of non-proliferating, non-maturating quiescent cells were implemented (Q1 and Q2). Thus, two additional parameters were estimated: F_{prol}, which was the fraction of cells proliferating entering the maturation chain and not transitioning to the quiescent stages, and k_{cycle}, the circulation rate constant within the quiescent cell cycle.

For physiological plausibility, **Model C** (Fig 1C) was additionally newly developed that mimicked also slowly replicating pluripotent stem cells in the bone marrow as a prior additional compartment (“Stem”)

in the chain of granulopoiesis. Their proliferation was controlled by a different proliferation rate constant (k_{stem}). Model C was described by the following set of ordinary differential equations:

$$\frac{dStem}{dt} = k_{stem} \cdot \left(1 - E_{drug}(t)\right) \cdot FB \cdot Stem - k_{stem} \cdot Stem \quad (4)$$

$$\frac{dProl}{dt} = k_{prol} \cdot \left(1 - E_{drug}(t)\right) \cdot FB \cdot Prol - k_{tr} \cdot Prol + k_{stem} \cdot Stem \quad (5)$$

$$\frac{dTransit1}{dt} = k_{tr} \cdot Prol - k_{tr} \cdot Tranisit1 \quad (6)$$

$$\frac{dTransit2}{dt} = k_{tr} \cdot Transit1 - k_{tr} \cdot Tranisit2 \quad (7)$$

$$\frac{dTransit3}{dt} = k_{tr} \cdot Transit2 - k_{tr} \cdot Tranisit3 \quad (8)$$

$$\frac{dCirc}{dt} = k_{tr} \cdot Transit3 - k_{tr} \cdot Circ \quad (9)$$

in which Stem, Prol, Transit1, Transit2, Transit3 and Circ represent different stages of granulopoiesis. Both proliferation rate constants (k_{prol} and k_{stem}) were affected by the same PD parameter (SL) and feedback mechanism. To ensure homeostasis of the system without therapy, k_{prol} was estimated as a fraction f_{tr} of the transition rate constant k_{tr}:

$$k_{prol} = f_{tr} \cdot k_{tr} \quad (10)$$

$$k_{stem} = (1 - f_{tr}) \cdot k_{tr} \quad (11)$$

Hence, f_{tr} is the fraction of k_{prol} (f_{tr}) and k_{stem} (i.e. the remaining fraction ($1-f_{tr}$)) of the sum of both input processes for Prol – and due to equilibration – the corresponding fractions of k_{tr}. Thus, f_{tr} determines the ratio between k_{stem} and k_{prol} ($k_{stem}/k_{prol}=(1-f_{tr})/f_{tr}$). As approximations, if f_{tr} is estimated >0.5, then k_{stem} becomes smaller than $k_{prol;}$ oppositely, if $f_{tr}=1$, then $k_{stem}=0$ which would result in the original Friberg *et al.* model. This parametrization enabled that k_{tr} could still be computed as in the original Friberg *et al.* model, by estimating MMT.

To describe baseline neutrophil concentrations, individual pretreatment concentrations were used allowing for residual variability ("baseline method 2" (Dansirikul *et al.*, 2008)). This individual baseline value ($Circ_0$) was also the initial condition for all PD compartments of the differential equations in all PK/PD models (i.e. $Stem(t_0)=Prol(t_0)=Transit1(t_0)=Transit2(t_0)=Transit3(t_0)=Circ(t_0)=Circ_0$), except in Model B for Prol ($Prol(t_0)= Circ_0/F_{prol}$) and the quiescent cell compartments ($Q1(t_0)=Q2(t_0)=(1-F_{prol})\bullet Prol(t_0)$) as described in (Mangas-Sanjuan *et al.*, 2015). If two measurements were available before the 1st drug administration (baseline visit and 1st day of 1st cycle), the mean of the two values was used as individual neutrophil baseline. In addition for Model C, other baseline methods suggested by Dansirikul *et al.* were investigated. Further, an Emax model was evaluted, instead of a linear relation

between drug concentration and drug effect. Finally, the number of transit compartments was varied and investigated.

An exponential model was applied for the interindividual variability as well as for the residual variability. First-order conditional estimation method with interaction was used for the 3 models.

Comparing Model A-C: model evaluation and model performance

Model evaluation and selection was based on parameter precision (relative standard error, RSE), condition number (ratio of highest to lowest eigenvalue of the correlation matrix), goodness-of-fit plots of individual predictions, population predictions and weighted residuals as well as on pcVPCs. Further, the Akaike Information Criterion (AIC=OFV+2•k; in which OFV is the objective function value and k is the number of model parameter estimates) was used, if models were not nested. In addition, physiological plausibility was considered to ensure reliable extrapolations for subsequent simulations of different dosing scenarios.

Deterministic simulations were performed to explore the performance of Model A-C for a typical patient (male, 56 years, total bilirubin concentration: 7 µmol/L, BSA: 1.8 m², baseline neutrophil concentration: $6.48 \cdot 10^9$ cells/L (= median baseline of males, experimental arm)) undergoing 3-weekly dosing of 185 mg/m² for 6 cycles using the typical parameter estimates of each model. Cell concentrations not only in the circulating cell compartment, but for all compartments were explored. For Model A, the second drug effect was either assumed to be active only until the end of the last cycle (3 weeks after the last dose administration) or to continue beyond the end of observation period.

The relative change of the highest and the lowest neutrophil concentration (nadir) from the 1st to the 6th cycle of each model was calculated based on this deterministic simulation and used to quantify cumulative neutropenia:

$$\text{Relative change of maximum value, \%} = 100 - \left(\frac{max.\ concentration\ at\ beginning\ of\ 6^{th}\ cycle}{baseline\ concentration} \cdot 100\right) \quad (12)$$

$$\text{Relative change of nadir value, \%} = 100 - \left(\frac{nadir\ concentration\ in\ 6^{th}\ cycle}{nadir\ concentration\ in\ 1^{st}\ cycle} \cdot 100\right) \quad (13)$$

Differentiation between the effect of paclitaxel and the platinum-based drugs

Model C was eventually further optimized by considering the combination of paclitaxel with carbo- or cisplatin. None of the patients received carbo- and cisplatin within one cycle. However, some of the patients receiving cisplatin were switched to carboplatin during the treatment. To account for both

platinum-based drugs, two published structural and covariate PK models (de Jongh *et al.*, 2004; Lindauer *et al.*, 2010) were integrated. Since no drug concentration measurements were available, variability was neglected. Thus, the typical concentration time-profiles of carbo- and cisplatin, respectively, were retrieved and these population predictions were used to estimate two additional slope factors for carbo- and cisplatin. An additive drug effect was assumed for the combination therapy.

$$E_{drug} = SL_{Platin} \cdot C_{Platin}(t) + SL \cdot C_{PTX}(t) \quad (14)$$

in which SL_{Platin} and $C_{Platin}(t)$ are the slope factor and the plasma concentration at time t of the co-administered platinum-based drugs, respectively.

This combination PK/PD model was evaluated as described for Model A-C. In addition, as described for the original PK/PD model, an external model evaluation was performed using the data from the conventional study arm. For this step, a pcVPC was generated, simulating 1000 datasets with the combination PK/PD model (in a simultaneous PK/PD analysis) considering interindividual variability in the PK and PD parameters.

Software for data analysis

All modelling and simulation activities were performed in NONMEM (version 7.3; Icon Development Solutions, Ellicott City, MD, USA) in combination with PsN (version 4.4.0), while dataset preparation and analysis of results were performed in R (version 3.2.2) including vpc R package (version 0.1.1). Deterministic simulations were done in Berkeley Madonna (version 8.3.18; Macey IE & Oster GF, UC Berkeley, CA, USA).

JPET Fast Forward. Published on June 9, 2017 as DOI: 10.1124/jpet.117.240309
This article has not been copyedited and formatted. The final version may differ from this version.

6 Results

Data analysis: CEPAC-TDM Study

The two different dosing strategies of the two study arms led to a higher median paclitaxel dose of 315 mg in the conventional arm (range: 205-438 mg) vs 270 mg (range: 111-505 mg) in the experimental arm. In addition to paclitaxel, patients received a platinum-based drug, primarily carboplatin (149 vs 33 in the conventional and 153 vs 30 in experimental arm, respectively). From those 63 patient in the cisplatin group, 9 were switched to carboplatin co-treatment during the therapy, due to cisplatin-related toxicity.

A total of 658 paclitaxel PK samples were obtained from the experimental arm (no PK measurements available from the conventional arm), while 1635 and 1639 PD measurements were available from the conventional and experimental arm, respectively.

External PK model evaluation and optimization using prior information

Paclitaxel concentrations from the CEPAC-TDM clinical trial were used to evaluate the original PK model for its applicability to the present data. This external PK model evaluation showed a good prediction of the individual measurements (Supplemental Figure 2). However, high shrinkage was observed (for interindividual variability: VM_{EL}: 47.4%; Km_{TR}: 92.9%; VM_{TR}: 92.3%; k_{21}: 97.6%; V_3: 58.5%; Q: 52.8%; for interoccasion variability: V_1: 98.6%; VM_{EL}: 57.2%; residual variability: 97.4%). Moreover, underprediction of the paclitaxel plasma concentrations was observed at the population level (pcVPC, Figure 2A), especially in the relevant target concentration range of 0.05 µmol/L.

To account for the observed misspecification and to improve the predictivity of the PK model, the MAP Bayesian approach (Gisleskog *et al.*, 2002) was applied combining the original PK parameter estimates (Table 1, 2nd column) as prior information with the newly obtained CEPAC-TDM data. For most of the parameters, only slight differences in the newly estimated PK parameter were observed compared to the original PK parameters. However, residual variability and two fixed-effects parameters, Km_{EL} (concentration at half of the maximum elimination capacity) and the covariate effect of bilirubin, were outside the 95% confidence interval of the original PK model, although with overlapping confidence intervals. Covariate parameters in general were estimated to be less influential on VM_{EL}. The highest relative changes in the parameter estimates were observed for the volume of distribution of the 2nd peripheral compartment (V_3) and for the intercompartmental clearance between central and

JPET Fast Forward. Published on June 9, 2017 as DOI: 10.1124/jpet.117.240309
This article has not been copyedited and formatted. The final version may differ from this version.

2nd peripheral compartment (Q) (+9.5% and +7.7%, respectively), even though they were still within the 95% confidence interval of the original parameters. The higher estimates of V_3 and Q translated into a larger paclitaxel distribution to the 2nd peripheral compartment and a reduced distribution back to the central compartment. These, together with a lower elimination (due to increased Km_{EL}) led to higher predicted paclitaxel concentrations, especially in the later phases of the concentration-time profile resulting in higher exposure. These changes in the PK parameters resulted in an improved description of the paclitaxel concentration time-profiles as illustrated in Figure 2B.

Aside from the population level, differences in the individual prediction resulting from the two PK parameter sets (original and optimized) were assessed by comparing their EBEs and individual exposure parameters (Figure 2C): For EBEs V_3 showed the highest difference in the EBEs ($MRPE_p$: -14.7%) while overall higher individual exposure estimates of $T_{C>0.05}$ and AUC ($MRPE_p$: -5.82% and -4.28%, respectively) were revealed for the optimized PK model.

External PK/PD model evaluation

Subsequently, the EBEs obtained with the optimized PK model were used to predict the individual PK concentration-time profiles, which eventually informed the PD response using the original PD parameters of the Friberg *et al.* model. This PK/PD model overpredicted the neutrophil concentrations (thus, underpredicted severity of neutropenia) during the whole observed period (pcVPC, Figure 3A); overprediction was already present for day 15 values in the 1st cycle, and increased for the measurements of day 1 and day 15 over the cycles. While the cumulative neutropenia led to decreasing neutrophil concentrations on day 1 and 15 over the cycles, the model predicted increasing neutrophil concentrations on day 15 instead since the dose was reduced during therapy. This led to an increasing discrepancy between observed neutrophil data and model prediction over time.

PK/PD model optimization

To better describe cumulative neutropenia over repeated treatment cycles the PD part was optimized. The performance and behavior of 3 different structural PK/PD models, two from literature (Model A and B, Figure 1A and B) and one newly developed for physiological plausibility (Model C, Figure 1C), were evaluated.

Parameters of all models were estimated with high precision (RSE<15%) (Table 2, column 1-5), except 2 parameters for Model B (SL and k_{cycle}; RSE>25%). Overparameterisation was detected for none of the

JPET Fast Forward. Published on June 9, 2017 as DOI: 10.1124/jpet.117.240309
This article has not been copyedited and formatted. The final version may differ from this version.

models (condition number <130). AIC favored Model C being lowest (>100 points difference to Model A and B), followed by Model A and B.

Slope factors between the 3 models were highly variable, with the highest value for Model B. In addition, the interindividual variability on SL was the highest for this model. For Model A, the estimated frB implied that $BASE_{tot}(t)$ decreased exponentially to approximately 50% of its original $BASE_{tot}(t_0)$ (half-life ≈15 days, based on k_{depl} and assuming $T_{C>0.05}$ to be 30 h) which was the trigger for homeostasis and affected all cell compartments. For Model B, the estimates of F_{prol} and k_{cycle} indicated that approximately 30% of the cells in Prol continued the maturation process, while 70% underwent the additional circulation as quiescent cells. In this circulation, the mean transition time was 43.3 h (=3/k_{cycle}). The estimate of f_{tr} in Model C (determining k_{stem} and k_{prol} as fraction of k_{tr}) expressed that the replication in Stem was approximately 73% slower than in Prol. Interindividual variability on the MMT was negligible in the optimized PK/PD models, due to small estimates (coefficient of variation <10%) and high η-shrinkage (>50%).

The pcVPCs (Figure 3B-D) showed that all 3 PK/PD models captured some of the observed pattern of cumulative neutropenia, but to a different extent. Model A and C described the observed neutrophil concentrations similarly well compared to Model B, especially in the later cycles.

Further, Model C was not improved by implementation of an Emax model compared to a linear drug effect model. In addition, different baseline methods and variations in the number of transit compartments were explored but did not improve the model in terms of objective function value, parameter precision goodness-of-fit plots and pcVPCs.

Regarding the deterministic simulation with constant doses of 185 mg/m² for 6 cycles (Figure 4), Model A predicted approximately the same maximum value for the 1st cycle (baseline) and the 2nd cycle; thereafter, the relative change of maximum value over all 6 cycles was the highest (31.4%) comparing Model A-C. The relative change of nadir value (36.5%) was in between Model B and C. Model B predicted the lowest degree of cumulative neutropenia (relative change of nadir and maximum value: 7.65% and 17.0%, respectively), despite the most significant initial relative change in the maximum value from the 1st to the 2nd cycle; afterwards the maximum value was not changing further. Model C predicted a relative change of the maximum value of 27.6% which was between Model A and B; at the same time, the highest cumulative neutropenia effect for the nadir value (relative change of the nadir value: 67.8%) was observed. This high degree of cumulative neutropenia resulted in grade 2 neutropenia for the 1st cycle, grade 3 from the 2nd and grade 4 from the 5th cycle on. For concentrations

JPET Fast Forward. Published on June 9, 2017 as DOI: 10.1124/jpet.117.240309
This article has not been copyedited and formatted. The final version may differ from this version.

in the stem cell compartment of Model C, recovery was not achieved within a cycle of 3 weeks length (Supplemental Figure 3).

Predictions of the 3 PK/PD models using deterministic simulation for neutrophil values after the end of the 6th treatment cycle varied substantially (Figure 4). For Model A, two possibilities regarding how to handle the second drug effect were investigated: either considering E_{drug2} only during the 6 cycles (18 weeks) or that it continued after treatment. If continued, $BASE_{tot}(t)$ did not recover and the pre-treatment baseline was not reached again. If not continued after 18 weeks, the original baseline was reached approximately 5 weeks after the last dose. Model B also showed a fast recovery of the neutrophil concentration to the pre-treatment baseline with almost no oscillation (within 3 weeks after end of cycle 6), even though the γ exponent of the feedback function was the highest. This might be caused by reduced proportion of cells entering the maturation chain. All models (except if continuation of E_{drug2} in Model A is assumed) predicted that baseline would be reached after end of therapy, but the time required was longer for Model C (approximately half a year after the last drug administration), while for Model A (assumption of no E_{drug2} after last cycle) and Model B baseline was reached again after approximately 5 weeks after the last dose. Overall the deterministic simulation of Model C showed the most physiological prediction, given that baseline recovery in Model A was dependent on the assumption taken for $E_{drug2,}$ and Model B predicted a decrease in the neutrophil concentrations only for the 1st cycle. In summary, even though all models described the observed cumulative neutropenia, the deterministic simulation of Model C was the most plausible and the model performance was also superior regarding the AIC.

Differentiation between the effect of paclitaxel and the platinum-based drugs

Model C was further expanded to distinguish between the drug effect of paclitaxel and platinum-based drugs. Based on the pcVPCs (Figure 3E), the performance was similar to Model C, nevertheless the AIC dropped 42.5 points. Parameters were estimated with sufficient precision (RSE<20%) for all parameters, but those of the slope factors slightly increased (RSE: 16.9%, 26.1%; Table 2, right column). The condition number (113) did not indicate an overparameterisation of the model. Estimated system PD parameters remained within the range of those of Model C. Only the drug effect of paclitaxel was reduced by 60.5% compared to Model C, given that the effect was now split into two effects, for paclitaxel and the platinum-based drugs. Interindividual variability on the slope factor of paclitaxel was increased compared to Model C. While the slope factor of carboplatin was estimated in a reasonable range, the

slope factor of cisplatin was implausibly high (32.1 L/mg), very likely due to the low number of patients (n=33) treated with this drug. Hence, dose individualization based on this model should be only recommended for the combination of paclitaxel with carboplatin.

Finally, the optimized PKPD platinum combination model, including separate drug effects for paclitaxel and the platinum-based drugs was used to predict the neutrophil concentration-time profiles of the conventional study arm of the CEPAC-TDM study (pcVPC, Figure 3F). A good prediction of the median and 95th percentile was achieved, although an underprediction of the low concentration-time profiles (5th percentile) was visible but still predicted the same neutropenia grade.

7 Discussion

Due to the narrow therapeutic window and the high interindividual PK and PD variability of paclitaxel, model-based dose individualization can help to reduce toxicity without compromising efficacy, as in a first step shown for neuropathy in the CEPAC-TDM study (Joerger *et al.*, 2016) but not for neutropenia. To further improve therapy for patients suffering from severe neutropenia, we evaluated, optimized and expanded the PK/PD model on which the dosing algorithm for the CEPAC-TDM study was developed. Thus, the Friberg *et al.* neutropenia PK/PD model was extended to describe cumulative neutropenia after repeated chemotherapy cycles in combination with cis-/carboplatin.

The individual PK predictions of the original model matched the paclitaxel concentrations measured in the CEPAC-TDM study well, due to the sparse sampling and the high interindividual variability in the model. However, an underprediction was observed when evaluating the population level, pointing towards suboptimal original PK parameter values for the investigated population. Since PK/PD modelling was undertaken sequentially, PK misspecifications may also affect PD. Therefore, PK model optimization was performed using the MAP Bayesian approach (Gisleskog *et al.*, 2002). The re-estimated parameters described the paclitaxel concentrations in the terminal phase of the concentration-time profile better by a faster distribution to the 2nd peripheral compartment and slower elimination. Further, the optimized PK parameter set predicted higher exposure for the population and the individuals. Overall, the re-estimated PK parameters were in line with parameters previously published (high volume of distribution (>100 L) (Gianni *et al.*, 1995; van Zuylen *et al.*, 2001); fast elimination (clearance >30 L/h) (Wiernik *et al.*, 1987; van Zuylen *et al.*, 2001)) and improved the predictive performance. Thus, the re-estimated PK parameters were used for the following steps.

An external evaluation of the Friberg *et al.* neutropenia model was performed with two major findings: First, overprediction of neutrophil concentrations at day 15, i.e. less toxic effect on neutrophils, already in the 1st cycle, pointed towards the need of a higher slope factor. Second, cumulative neutropenia, which was not accounted for in the Friberg *et al.* model but is often seen in clinical practice after repeated cycles with cytotoxic drugs, but only rarely investigated. We hypothesized that this pattern was caused by bone marrow exhaustion (BME) due to the damage of early primitive bone marrow stem cells, such as pluripotent long-term haematopoietic stem cells (Mauch *et al.*, 1995).

Since the Friberg *et al.* model for neutropenia predicted approximately the same nadir concentration and, thus, extent of neutropenia for each cycle if doses were kept constant, the original model was not

capable of describing the observed cumulative neutropenia and signs of BME during repeated chemotherapy cycles. Three different structural models were investigated (Model A-C) to improve the predictivity of the PK/PD model for long-term treatment, as in the CEPAC-TDM study. Model A (adapted from Bender *et al.*, 2012) followed a more empirical approach: by decreasing a part of $BASE_{tot}(t)$ time-dependently, the feedback effect and therewith the recovery of the neutrophil concentration was reduced. Initially, Model B (adapted from Mangas-Sanjuan *et al.*, 2015) was not intended for describing cumulative myelosuppression, but thrombocytopenia after different dosing schedules. Nevertheless, this model predicted lower neutrophil concentrations than the Friberg *et al.* model for repeated dosing. Model B used a more mechanistic approach by implementing two stages of quiescent cells accounting for progenitor cells that can potentially replicate but rest and therefore are not harmed by the treatment (comparable to G_0 phase in cell cycle). Finally, a new model, Model C, was developed to implement the BME hypothesis by adding a stem cell compartment as first compartment in the maturation chain. In accordance with physiology, proliferation of the stem cells was slower (73%) but was affected by the same drug- and feedback effect as cells in Prol.

All three PK/PD models were successfully implemented and parameters were estimated with high precision. The slope factor of these models was estimated to be higher than in the original model, while high differences between them were observed but could not be compared across models due to differences in the implementation of the drug effect.

Cumulative neutropenia was described by all three models to a certain extent, however the potential for extrapolation of Model A and B may be limited. For Model A, the parameter estimate k_{depl} for the time-dependent effect is specific for the treatment cycle length of the underlying data and predictions after the end of treatment strongly depend on the assumptions for the duration of E_{drug2}. For Model B, full recovery and equilibrium was reached very quickly after the last dose. Thus, an increased cycle length would reduce or let disappear the cumulative effect which is often experienced by oncologists who then empirically reduce dosing (as in conventional study arm). Model C, on the other hand, described cumulative neutropenia in a more semi-mechanistic way supporting the BME hypothesis. For nadir and maximum values of the neutrophil concentrations, a decrease over the cycles was observed, but maximum values were more affected, as supported by the data. The inability of the stem cell compartment to recover within a cycle mimicked the aforementioned BME hypothesis that long-term stem cells are damaged. Note that although proliferation of stem cells was affected by the same drug effect parameter ($E_{drug}=SL \bullet C_{PTX}(t)$), the overall toxic effect for each of the two cell types in bone marrow

JPET Fast Forward. Published on June 9, 2017 as DOI: 10.1124/jpet.117.240309
This article has not been copyedited and formatted. The final version may differ from this version.

is dependent on the proliferation rate (i.e. k_{prol}•(1-E_{drug}) and k_{stem}•(1-E_{drug})) (Berenbaum, 1972) which is smaller for stem cells compared to progenitor cells (Steinman, 2002). Hence, stem cells were ultimately assumed to be less susceptible in accordance with literature (Harrison and Lerner, 1991). Damage of these cells was especially seen for the second and following cytotoxic dose administrations, when due to the haematopoietic stress caused by the first drug administration, the stem cell proliferation was stimulated, thus, being more vulnerable (Harrison and Lerner, 1991; Trumpp *et al.*, 2010). The BME hypothesis is also supported by the fact that the platelet concentrations showed the same decreasing pattern over time (Supplemental Figure 4), which is plausible when the stem cells, from which neutrophils and platelets originate, are disturbed. Model C further predicted a long span (approx. half a year after last dose) for the stem cells to fully recover. Since no neutrophil measurements were available for such a long period, the hypothesized long recovery time for the entire bone marrow beyond the 6th cycle represent extrapolations needing further validation. Unfortunately, this period is typically not monitored even though baseline is not achieved, since the patients rapidly recovery to non-neutropenic grade 0. Nevertheless, a long recovery time seems plausible, since previous chemotherapies have been identified to reduce baseline (Kloft *et al.*, 2006), supporting the assumption that the bone marrow could still be affected. Model C also showed good agreement of the system-related parameters (MMT and γ) between the original model and literature (Friberg *et al.*, 2002), indicating that previous knowledge gained from the Friberg *et al.* model, could be used to inform Model C. Overall, the best description of the neutrophil data was obtained using Model A and Model C. However, Model C integrated the most physiological explanation for the effect and has the potential to describe long-term treatment with paclitaxel.

So far, only the neutropenic effect of paclitaxel had been considered, but combination therapy with cis-/carboplatin, known to have an impact on neutropenia (Go and Adjei, 1999), was administered. Differentiation of drug effects was necessary for future simulation, when dose recommendation of paclitaxel and the platinum-based components shall be adapted. Thus, Model C was extended and the platinum combination model assuming additive drug effects slightly improved the model prediction, while allowing for a more realistic drug effect.

The estimated paclitaxel slope in the combination PK/PD model was lower than in Model C, which is reasonable since the drug effect was divided into two components (paclitaxel and platinum-based drugs). Compared to literature, paclitaxel and carboplatin slope factors were approximately 2-fold higher as previously reported for the respective monotherapy (paclitaxel: 2.21 L/µmol (Friberg *et al.*, 2002),

1.85 L/µmol (Joerger *et al.*, 2007); carboplatin: 0.460 L/mg (Schmitt *et al.*, 2010)). Deviations point towards a synergistic pharmacodynamic interaction, which is not considered in the additive assumption underlying this model. Synergism has been suggested previously (Choy *et al.*, 1998; Engblom *et al.*, 1999) and is mechanistically plausible: paclitaxel increases the proportion of cells in G_1 phase of the cell cycle, where cells become more sensitive to carboplatin (Long and Fairchild, 1994; Engblom *et al.*, 1999). However, more complex models (e.g. general PD interaction model (Wicha *et al.*, 2016)) were not supported by the data. Hence, the simplified (additive effect model) was selected, but predictions of neutropenia grade from extrapolated combination drug concentrations should be regarded with care, since the synergistic interaction depends on both drug concentrations. Despite this limitation, the platinum combination model well described the data also from the conventional study arm, indicating good predictive performance.

To conclude, a comprehensive PK/PD model able to describe and predict cumulative neutropenia after paclitaxel combination therapy was developed. Describing this long-term effect semi-mechanistically improved the understanding of neutropenia and gave further evidence of the BME hypothesis that the effect on the pluripotent stem cells might cause cumulative neutropenia. Due to the mechanistic character of the model, the framework can be applied to other myelotoxicity drugs. In addition, the model can differentiate between the paclitaxel and carboplatin effect which allows for better predictions of dose adaptations for patients with non-small cell lung or ovarian cancer. Further data assessment with other doses of the combination therapy as well as neutrophil concentration evolvement after treatment end should be performed. This model showed a high predictive performance for the conventional arm in which no drug concentration had been determined. In this work we used a confirmatory phase IV study not only for assessing the dosing algorithm but also for additional learning, as suggested by (Sheiner *et al.*, 1997).The developed paclitaxel-carboplatin combination PK/PD model laid the basis for further explorations of different dosing strategies to increase our knowledge and thus to contribute to further individualized anticancer treatment.

8 Acknowledgements

The authors thank the High-Performance Computing Service of ZEDAT at Freie Universitaet Berlin (http://www.zedat.fuberlin.de/Compute) for computing time; the Central European Society of Anticancer Drug Research (CESAR) for providing the study data and Dr. Niklas Hartung for discussions about prior information.

9 Authorship Contributions

Performed data analysis: Henrich

Participated in research/analysis design: Henrich, Parra-Guillen, Kloft, Joerger, Huisinga

Wrote or contributed to the writing of the manuscript: Henrich, Parra-Guillen, Kloft, Joerger, Huisinga, Jaehde, Kraff

10 References

Bauer RJ (2014) NONMEM user guide - introduction to NONMEM 7.3.0, Hanover, Maryland.

Bender BC, Schaedeli-Stark F, Koch R, Joshi A, Chu Y-W, Rugo H, Krop IE, Girish S, Friberg LE, and Gupta M (2012) A population pharmacokinetic/pharmacodynamic model of thrombocytopenia characterizing the effect of trastuzumab emtansine (T-DM1) on platelet counts in patients with HER2-positive metastatic breast cancer. *Cancer Chemother Pharmacol* **70**:591–601.

Berenbaum MC (1972) In vivo determination of the fractional kill of human tumor cells by chemotherapeutic agents. *Cancer Chemother reports* **56**:563–571.

Bergstrand M, Hooker AC, Wallin JE, and Karlsson MO (2011) Prediction-corrected visual predictive checks for diagnosing nonlinear mixed-effects models. *AAPS J* **13**:143–151.

Choy H, Akerley W, and Devore R (1998) Paclitaxel, carboplatin and radiation therapy for non-small-cell lung cancer. *Oncology (Williston Park)* **12**:80–86.

Dansirikul C, Silber HE, and Karlsson MO (2008) Approaches to handling pharmacodynamic baseline responses. *J Pharmacokinet Pharmacodyn* **35**:269–283.

de Jongh FE, Gallo JM, Shen M, Verweij J, and Sparreboom A (2004) Population pharmacokinetics of cisplatin in adult cancer patients. *Cancer Chemother Pharmacol* **54**:105–112.

Efron B, and Tibshirani R (1986) Bootstrap methods for standard errors, confidence intervals, and other measures of statistical accuracy. *Stat Sci* **1**:54–77.

Engblom P, Rantanen V, Kulmala J, and Grènman S (1999) Carboplatin-paclitaxel- and carboplatin-docetaxel-induced cytotoxic effect in epithelial ovarian carcinoma in vitro. *Cancer* **86**:2066–2073.

Friberg LE, Henningsson A, Maas H, Nguyen L, and Karlsson MO (2002) Model of chemotherapy-induced myelosuppression with parameter consistency across drugs. *J Clin Oncol* **20**:4713–4721.

Gianni L, Kearns CM, Giani A, Capri G, Viganó L, Lacatelli A, Bonadonna G, and Egorin MJ (1995) Nonlinear pharmacokinetics and metabolism of paclitaxel and its pharmacokinetic/pharmacodynamic relationships in humans. *J Clin Oncol* **13**:180–190.

Gisleskog PO, Karlsson MO, and Beal SL (2002) Use of prior information to stabilize a population data analysis. *J Pharmacokinet Pharmacodyn* **29**:473–505.

Go RS, and Adjei AA (1999) Review of the comparative pharmacology and clinical activity of cisplatin and carboplatin. *J Clin Oncol* **17**:409–422.

Gurney H (1996) Dose calculation of anticancer drugs: a review of the current practice and introduction

of an alternative. *J Clin Oncol* **14**:2590–2611.

Harrison DE, and Lerner CP (1991) Most primitive hematopoietic stem cells are stimulated to cycle rapidly after treatment with 5-fluorouracil. *Blood* **78**:1237–1240.

Huizing MT, Giaccone G, van Warmerdam LJ, Rosing H, Bakker PJ, Vermorken JB, Postmus PE, van Zandwijk N, Koolen MG, ten Bokkel Huinink WW, van der Vijgh WJ, Bierhorst FJ, Lai A, Dalesio O, Pinedo HM, Veenhof CH, and Beijnen JH (1997) Pharmacokinetics of paclitaxel and carboplatin in a dose-escalating and dose-sequencing study in patients with non-small-cell lung cancer. The European Cancer Centre. *J Clin Oncol* **15**:317–329.

Huizing MT, van Warmerdam LJ, Rosing H, Schaefers MC, Lai A, Helmerhorst TJ, Veenhof CH, Birkhofer MJ, Rodenhuis S, Beijnen JH, and ten Bokkel Huinink WW (1997) Phase I and pharmacologic study of the combination paclitaxel and carboplatin as first-line chemotherapy in stage III and IV ovarian cancer. *J Clin Oncol* **15**:1953–1964.

Joerger M, Huitema ADR, Huizing MT, Willemse PHB, de Graeff A, Rosing H, Schellens JHM, Beijnen JH, and Vermorken JB (2007) Safety and pharmacology of paclitaxel in patients with impaired liver function: a population pharmacokinetic-pharmacodynamic study. *Br J Clin Pharmacol* **64**:622–633.

Joerger M, Huitema ADR, Richel DJ, Dittrich C, Pavlidis N, Briasoulis E, Vermorken JB, Strocchi E, Martoni A, Sorio R, Sleeboom HP, Izquierdo MA, Jodrell DI, Calvert H, Boddy A V, Hollema H, Féty R, Van der Vijgh WJF, Hempel G, Chatelut E, Karlsson M, Wilkins J, Tranchand B, Schrijvers AHGJ, Twelves C, Beijnen JH, and Schellens JHM (2007) Population pharmacokinetics and pharmacodynamics of paclitaxel and carboplatin in ovarian cancer patients: a study by the European organization for research and treatment of cancer-pharmacology and molecular mechanisms group and new drug development group. *Clin Cancer Res* **13**:6410–6418.

Joerger M, Kraff S, Huitema ADR, Feiss G, Moritz B, Schellens JHM, Beijnen JH, and Jaehde U (2012) Evaluation of a pharmacology-driven dosing algorithm of 3-weekly paclitaxel using therapeutic drug monitoring: a pharmacokinetic-pharmacodynamic simulation study. *Clin Pharmacokinet* **51**:607–617.

Joerger M, von Pawel J, Kraff S, Fischer JR, Eberhardt W, Gauler TC, Mueller L, Reinmuth N, Reck M, Kimmich M, Mayer F, Kopp H-G, Behringer DM, Ko Y-D, Hilger RA, Roessler M, Kloft C, Henrich A, Moritz B, Miller MC, Salamone SJ, and Jaehde U (2016) Open-label, randomized study of individualized, pharmacokinetically (PK)-guided dosing of paclitaxel combined with carboplatin or cisplatin in patients with advanced non-small-cell lung cancer (NSCLC). *Ann Oncol* **27**:1895–1902.

Kloft C, Wallin J, Henningsson A, Chatelut E, and Karlsson MO (2006) Population pharmacokinetic-pharmacodynamic model for neutropenia with patient subgroup identification: comparison across anticancer drugs. *Clin Cancer Res* **12**:5481–5490.

Lichtman SM, Hollis D, Miller AA, Rosner GL, Rhoades CA, Lester EP, Millard F, Byrd J, Cullinan SA, Rosen DM, Parise RA, Ratain MJ, Egorin MJ, and Cancer and Leukemia Group B (CALGB 9762) (2006) Prospective evaluation of the relationship of patient age and paclitaxel clinical pharmacology: Cancer and Leukemia Group B (CALGB 9762). *J Clin Oncol* **24**:1846–1851.

Lindauer A, Eickhoff C, Kloft C, and Jaehde U (2010) Population pharmacokinetics of high-dose carboplatin in children and adults. *Ther Drug Monit* **32**:159–168.

Long BH, and Fairchild CR (1994) Paclitaxel inhibits progression of mitotic cells to G1 phase by interference with spindle formation without affecting other microtubule functions during anaphase and telephase. *Cancer Res* **54**:4355–4361.

Mangas-Sanjuan V, Buil-Bruna N, Garrido MJ, Soto E, and Trocóniz IF (2015) Semimechanistic cell-cycle type-based pharmacokinetic/pharmacodynamic model of chemotherapy-induced neutropenic effects of diflomotecan under different dosing schedules. *J Pharmacol Exp Ther* **354**:55–64.

Mauch P, Constine L, Greenberger J, Knospe W, Sullivan J, Liesveld JL, and Deeg HJ (1995) Hematopoietic stem cell compartment: acute and late effects of radiation therapy and chemotherapy. *Int J Radiat Oncol Biol Phys* **31**:1319–1339.

Mielke S (2007) Individualized pharmacotherapy with paclitaxel. *Curr Opin Oncol* **19**:586–589.

Mitchison TJ (2012) The proliferation rate paradox in antimitotic chemotherapy. *Mol Biol Cell* **23**:1–6.

Ohtsu T, Sasaki Y, Tamura T, Miyata Y, Nakanomyo H, Nishiwaki Y, and Saijo N (1995) Clinical pharmacokinetics and pharmacodynamics of paclitaxel: a 3-hour infusion versus a 24-hour infusion. *Clin Cancer Res* **1**:599–606.

Savic RM, and Karlsson MO (2009) Importance of shrinkage in empirical bayes estimates for diagnostics: problems and solutions. *AAPS J* **11**:558–569.

Schmitt A, Gladieff L, Laffont CM, Evrard A, Boyer J-C, Lansiaux A, Bobin-Dubigeon C, Etienne-Grimaldi M-C, Boisdron-Celle M, Mousseau M, Pinguet F, Floquet A, Billaud EM, Durdux C, Le Guellec C, Mazières J, Lafont T, Ollivier F, Concordet D, and Chatelut E (2010) Factors for hematopoietic toxicity of carboplatin: refining the targeting of carboplatin systemic exposure. *J Clin Oncol* **28**:4568–4574.

Sheiner LB (1997) Learning versus confirming in clinical drug development. *Clin Pharmacol Ther* **61**:275–291.

Sheiner LB, and Beal SL (1981) Some suggestions for measuring predictive performance. *J Pharmacokinet Biopharm* **9**:503–512.

Smorenburg CH, Sparreboom A, Bontenbal M, Stoter G, Nooter K, and Verweij J (2003) Randomized cross-over evaluation of body-surface area-based dosing versus flat-fixed dosing of paclitaxel. *J Clin Oncol* **21**:197–202.

Steinman RA (2002) Cell cycle regulators and hematopoiesis. *Oncogene* **21**:3403–3413.

Trumpp A, Essers M, and Wilson A (2010) Awakening dormant haematopoietic stem cells. *Nat Rev Immunol* **10**:201–209, Nature Publishing Group.

van Zuylen L, Karlsson MO, Verweij J, Brouwer E, de Bruijn P, Nooter K, Stoter G, and Sparreboom A (2001) Pharmacokinetic modeling of paclitaxel encapsulation in Cremophor EL micelles. *Cancer Chemother Pharmacol* **47**:309–318.

Wicha S, Chen C, Clewe O, and Simonsson U (2016) A general pharmacodynamic interaction (GPDI) model, Lisbon.

Wiernik PH, Schwartz EL, Einzig A, Strauman JJ, Lipton RB, and Dutcher JP (1987) Phase I trial of taxol given as a 24-hour infusion every 21 days: responses observed in metastatic melanoma. *J Clin Oncol* **5**:1232–1239.

Zufía López L, Aldaz Pastor A, Aramendia Beitia JM, Arrobas Velilla J, and Giraldez Deiró J (2006) Determination of docetaxel and paclitaxel in human plasma by high-performance liquid chromatography: validation and application to clinical pharmacokinetic studies. *Ther Drug Monit* **28**:199–205.

JPET Fast Forward. Published on June 9, 2017 as DOI: 10.1124/jpet.117.240309
This article has not been copyedited and formatted. The final version may differ from this version.

11 Footnotes

a) Source of financial support:

C. K. and W. H. report grants from an industry consortium (AbbVie Deutschland GmbH & Co. KG, Boehringer Ingelheim Pharma GmbH & Co. KG, Grünenthal GmbH, F. Hoffmann-La Roche Ltd, Merck KGaA and SANOFI). CK reports grants from the Innovative Medicines Initiative-Joint Undertaking ("DDMoRe") and Diurnal Ltd.

b) Thesis information, citation of meeting abstracts where the work was previously presented:

Part of this work was presented at the following meetings: Henrich *et al.* (2016) Annual Meeting of the Deutsche Pharmazeutische Gesellschaft (DPhG); Henrich *et al.* (2015 and 2016) Annual Meeting of the Central European Society of Anticancer Drug Research (CESAR); Henrich *et al.* (2015 and 2016) Population Approach Group Europe (PAGE).

c) Person to receive reprint requests:

d) [6, 7] shared senior authorship

JPET Fast Forward. Published on June 9, 2017 as DOI: 10.1124/jpet.117.240309
This article has not been copyedited and formatted. The final version may differ from this version.

12 Figure Legends

Fig. 1. Schematic representation of the original PK and the investigated PD models A-C, for paclitaxel plasma concentration- and neutrophil-time profiles.

Colors: **Red:** observation compartments; **green**, **orange** and **blue:** link between PK and PD model as well as changes from original model for Model A-C, respectively.

PK compartments: **Central:** central paclitaxel compartment; **Per1** and **Per2:** 1st and 2nd peripheral compartment.

PK parameters: **k_{21}:** distribution rate constant between Central and Per1; **Km_{EL}:** paclitaxel concentration at half VM_{EL}; **Km_{TR}:** paclitaxel concentration at half VM_{TR}; **Q:** intercompartmental clearance between Central and Per2; **V_1:** central volume of distribution; **V_3:** volume of distribution of Per2; **VM_{TR}:** maximum transport capacity; **VM_{EL}:** maximum elimination capacity.

PD compartments: **Circ:** circulating neutrophil cell compartment; **Prol:** proliferating cell compartment; **Q1** and **Q2:** quiescent cell compartments in Model B; **Stem:** stem cell compartment in Model C; **Transit:** transit compartments (3 for Model A-C).

PD parameters implemented in all PD models: **Circ(t)** and **Circ(t_0):** concentration of circulating neutrophils at time t and at t=0, respectively; **FB:** feedback; **k_{prol}:** proliferation rate constant of cells in Prol; **k_{tr}:** transition rate constant of maturation chain; **MMT:** mean maturation time; **γ:** exponent of feedback function.

PD parameters specific for Model A: **$Base_1$**: baseline of proliferating cells not affected by depletion; **$Base_2$:** baseline proliferating cells affected by depletion; **$BASE_{tot}(t)$** and **$BASE_{tot}(t_0)$:** total baseline proliferating cells at time t and time=0, respectively; **frB:** fraction of $BASE_{tot}(t_0)$ not affected by depletion.

PD parameters specific for Model B: **F_{prol}:** fraction of proliferating cells entering maturation chain; **k_{cycle}:** circulation rate constant within quiescent cell cycle.

PD parameters specific for Model C: **f_{tr}:** fraction of input in Prol via replication in Model C; **k_{stem}:** proliferation rate constant of cells in Stem.

Drug effect: **$C_{PTX}(t)$:** paclitaxel plasma concentration at time t; **E_{drug}:** drug effect on k_{prol} and in Model C on k_{stem}; **E_{drug2}:** additional drug effect on $Base_2$ in Model A; **k_{depl}:** depletion rate constant of E_{drug2} in Model A; **SL:** slope factor of paclitaxel; **$T_{C>0.05}$:** time of C_{PTX} >0.05 µmol/L.

JPET Fast Forward. Published on June 9, 2017 as DOI: 10.1124/jpet.117.240309
This article has not been copyedited and formatted. The final version may differ from this version.

Fig. 2. PK model evaluation.

Prediction-corrected visual predictive check of Panel A) external model evaluation of original PK model and Panel B) of optimized PK model.

Blue circles: observed paclitaxel concentrations; red lines: median (solid), 5th, 95th percentiles (dashed) of observations; black lines: median (solid), 5th and 95th percentiles (dashed) of simulations; shaded areas: 90% confidence intervals of simulated percentiles.

Panel C): Box-Whisker plot of individual relative prediction error ($RPE_{p,i,o,}$ light grey) and absolute value of $RPE_{p,i,o}$ (dark grey) determined by *post-hoc* estimation from optimized PK model compared to the ones from original parameter set. For parameters V_3, VM_{TR}, Km_{TR}, k_{21} and Q: n=183 (patients), for parameters $T_{C>0.05}$, AUC, VM_{EL}, V_1: n=720 (treatment cycles).

$T_{C>0.05}$: time of paclitaxel concentration >0.05 µmol/L; AUC: area under plasma concentration-time curve; Km_{EL}: paclitaxel concentration at half maximum elimination capacity; V_1: central volume of distribution; V_3: volume of distribution of 2nd peripheral compartment; VM_{TR}: maximum transport capacity; Km_{TR}: paclitaxel concentration at half VM_{TR}; k_{21}: distribution rate constant between central and 1st peripheral compartment; Q: intercompartmental clearance between central and 2nd peripheral compartment.

Boxes: inter-quartile range (IQR), including median; whiskers: range from box hinge to highest/lowest value within 1.5•IQR; points: data beyond whiskers.

Fig. 3. Prediction-corrected visual predictive check of neutropenia PK/PD models.

Panel A) original PK/PD model; Panel B) Model A; Panel C) Model B; Panel D) Model C; Panel E) platinum combination model. Panel F) platinum combination model applied to conventional study arm.

Blue circles: observed neutrophil concentrations; red lines: median (solid), 5th, 95th percentiles (dashed) of observations; black lines: median (solid), 5th and 95th percentiles (dashed) of simulations; shaded areas: 90% confidence intervals of simulated percentiles.

JPET Fast Forward. Published on June 9, 2017 as DOI: 10.1124/jpet.117.240309
This article has not been copyedited and formatted. The final version may differ from this version.

Fig. 4. Deterministic simulation of neutropenia using Model A-C for a typical male patient.

Patient: age: 56 years, bilirubin: 7 µmol/L, body surface area: 1.8 m²; baseline neutrophil concentration: $6.48 \cdot 10^9$ cells/L

Dosing: 3-weekly administration of 185 mg/m² paclitaxel for 6 cycles.

Green solid line: Model A with assumption of end of second drug effect 3 weeks after last dose; green dashed line: Model A with assumption of continuation of second drug effect; orange line: Model B; blue line: Model C; red dashed lines: thresholds for grading neutropenia from grade 0 to 4.

JPET Fast Forward. Published on June 9, 2017 as DOI: 10.1124/jpet.117.240309
This article has not been copyedited and formatted. The final version may differ from this version.

13 Tables

Table 1: Parameter estimates of original PK model compared to PK parameters from re-estimation using prior information.

Parameter [unit]	*Estimate (95% confidence interval)*	
	Original PK model [a]	***Optimized PK model*** [b]
Fixed-effects parameter		
V_1 [L]	10.8 (9.99 – 11.6)	10.8 (10.7 – 10.8)
V_3 [L]	275 (245 – 305)	301 (292 – 311)
Km_{EL} [µmol/L]	0.576 (0.49 – 0.662)	0.667 (0.645 – 0.687)
VM_{EL} [µmol/h]	35.8 (32.5 – 39.1)	35.9 (35.1 – 36.6)
Km_{TR} [µmol/L]	1.43 (1.19 – 1.67)	1.44 (1.38 – 1.48)
VM_{TR} [µmol/h]	177 (166 – 188)	175 (174 – 176)
k_{21} [h^{-1}]	1.11 (1.04 – 1.18)	1.12 (1.11 – 1.13)
Q [L/h]	15.6 (14.0 – 17.2)	16.8 (16.5 – 17.1)
Covariate-parameter relation		
BSA on VM_{EL}	1.30 (1.05 – 1.55)	1.14 (1.06 – 1.25)
Sex on VM_{EL}	1.16 (1.07 – 1.25)	1.07 (1.03 – 1.10)
Age on VM_{EL}	-0.449 (-0.630 – -0.268)	-0.447 (-0.525 – -0.367)
BILI on VM_{EL}	-0.160 (-0.223 – -0.0973)	-0.0942 (-0.124 – -0.0648)
Interindividual variability		
V_3, CV%	46.2 (39.4 – 53.0)	42.2 (41.5 – 43.0)
VM_{EL}, CV%	17.8 (14.6 – 21.0)	16.0 (15.1 – 16.9)
Km_{TR}, CV%	69.8 (58.2 – 81.4)	68.9 (68.7 – 69.5)
VM_{TR}, CV%	28.7 (24.4 – 33.0)	28.3 (28.3 – 28.4)
k_{21}, CV%	9.31 (-1.18 – 19.8)	8.94 (8.85 – 9.06)
Q, CV%	45.8 (40.4 – 51.2)	42.5 (41.9 – 43.3)
Interoccasion variability		
V_1, CV%	37.3 (34.0 – 40.6)	37.3 (fixed)
VM_{EL}, CV%	15.2 (13.0 – 17.4)	15.2 (fixed)
Residual variability		
Exponential, CV%	18.2 (18.1 – 18.3)	17.8 (17.8 – 17.8)

CV%: coefficient of variation; V_1: central volume of distribution; V_3: volume of distribution of 2nd peripheral compartment; Km_{EL}: paclitaxel concentration at half VM_{EL}; VM_{EL}: maximum elimination capacity; Km_{TR}:

JPET Fast Forward. Published on June 9, 2017 as DOI: 10.1124/jpet.117.240309
This article has not been copyedited and formatted. The final version may differ from this version.

paclitaxel concentration at half VM_{TR}; VM_{TR}: maximum transport capacity; k_{21}: distribution rate constant between central and 1st peripheral compartment; Q: intercompartmental clearance between central and 2nd peripheral compartment; BSA: body surface area [m^2]; BILI: bilirubin plasma concentration [µmol/L].

[a] Confidence intervals based on standard errors of original model, assuming normal distribution.

[b] Confidence intervals based on bootstrap analysis (1000 bootstrap datasets, convergence rate: 96.5%).

JPET Fast Forward. Published on June 9, 2017 as DOI: 10.1124/jpet.117.240309
This article has not been copyedited and formatted. The final version may differ from this version.

Table 2: Parameter estimates of the PK/PD model investigated during model optimization

Parameter [unit]	***Estimate (RSE, %)***				
	Original model [a]	***Model A***	***Model B***	***Model C***	***Platinum combination model***
AIC	n.a.	276.340	323.703	174.577	132.063
Fixed-effects parameters					
MMT [h]	141	128 (2.04)	117 (4.80)	145 (2.65)	142 (2.94)
SL [L/µmol]	2.6	4.35 (4.84)	173 (26.8)	13.1 (4.56)	5.18 (26.1)
γ	0.2	0.244 (7.54)	0.615 (9.28)	0.257 (5.53)	0.274 (5.11)
frB	n.a.	0.453 (4.68)	n.a.	n.a.	n.a.
k_{depl} [h^{-2}]	n.a.	$9.04 \cdot 10^{-5}$ (17.9)	n.a.	n.a.	n.a.
F_{prol}	n.a.	n.a.	0.315 (13.4)	n.a.	n.a.
k_{cycle} [h^{-1}]	n.a.	n.a.	0.0924 (26.1)	n.a.	n.a.
f_{tr}	n.a.	n.a.	n.a.	0.787 (2.76)	0.723 (2.03)
SL_{Carbo} [L/mg]	n.a.	n.a.	n.a.	n.a.	0.997 (16.9)
Interindividual variability					
MMT, CV%	27.0	n.a.	n.a.	n.a.	n.a.
SL, CV%	44.9	47.1 (7.57)	97.0 (12.7)	44.8 (6.54)	68.0 (15.4)
SL_{Carbo}, CV%	n.a.	n.a.	n.a.	n.a.	44.4 (15.5)
Residual variability					
Exponential, CV%	31.6%	53.9 (3.53)	55.1 (3.38)	51.5 (3.61)	50.7 (3.71)

RSE: relative standard error; CV%: coefficient of variation; AIC: Akaike information criterion; n.a: not applicable.

MMT: mean maturation time; SL: slope factor of paclitaxel; γ: exponent of feedback function; frB: fraction of $BASE_{tot}(t_0)$ not affected by depletion in Model A; k_{depl}: depletion constant of second drug effect in in Model A; $T_{C>0.05}$: time of C_{PTX} >0.05 µmol/L; F_{prol}: fraction of proliferating cells entering maturation chain in Model B; k_{cycle}: circulation rate constant within quiescent cell cycle in Model B. f_{tr}: fraction of input in Prol via replication in Model C; SL_{Carbo}: slope factor of carboplatin.

[a] Parameter precision was not published originally

JPET Fast Forward. Published on June 9, 2017 as DOI: 10.1124/jpet.117.240309
This article has not been copyedited and formatted. The final version may differ from this version.

14 Figures

Fig. 1

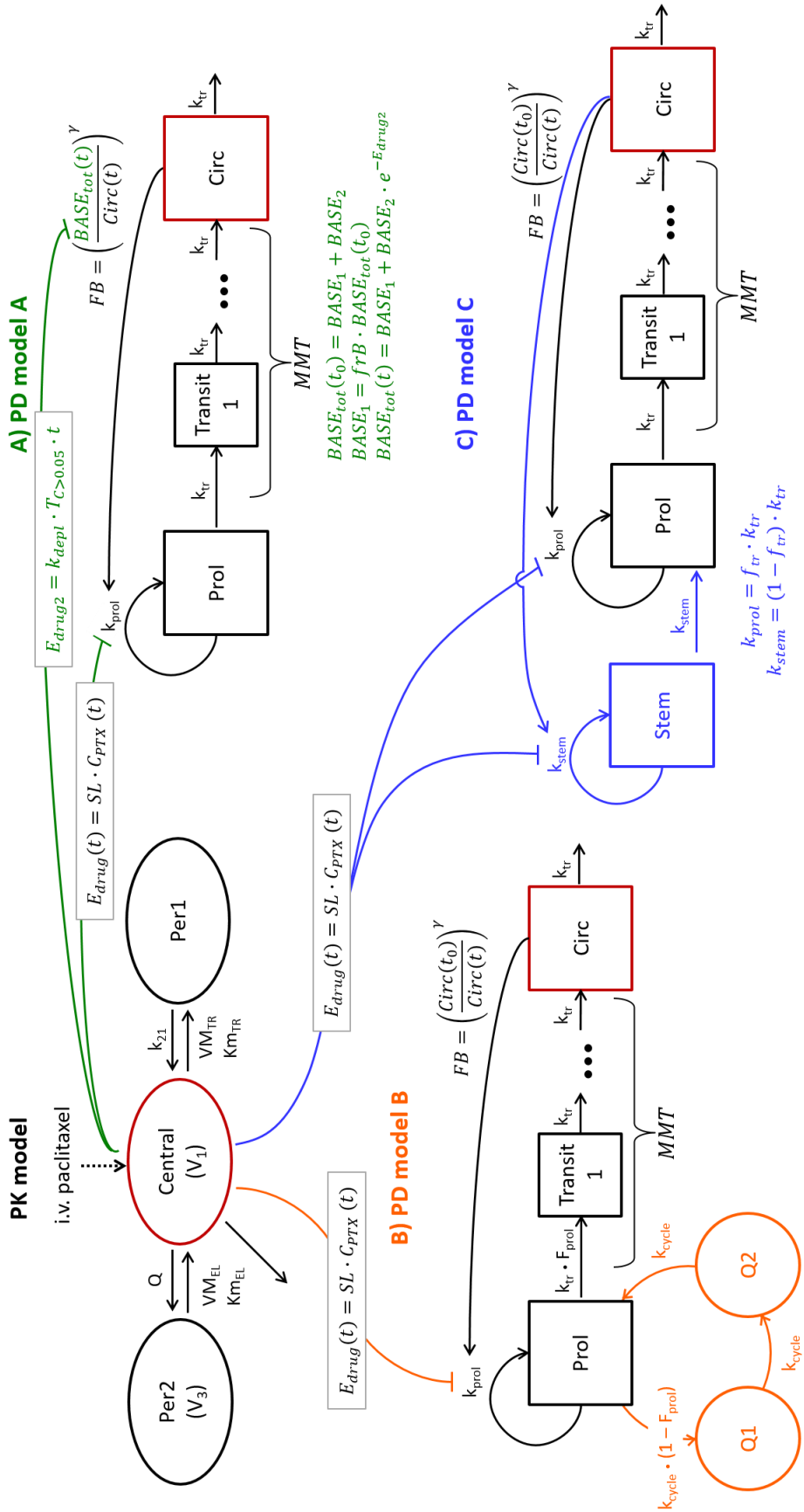

JPET Fast Forward. Published on June 9, 2017 as DOI: 10.1124/jpet.117.240309
This article has not been copyedited and formatted. The final version may differ from this version.

Fig. 2

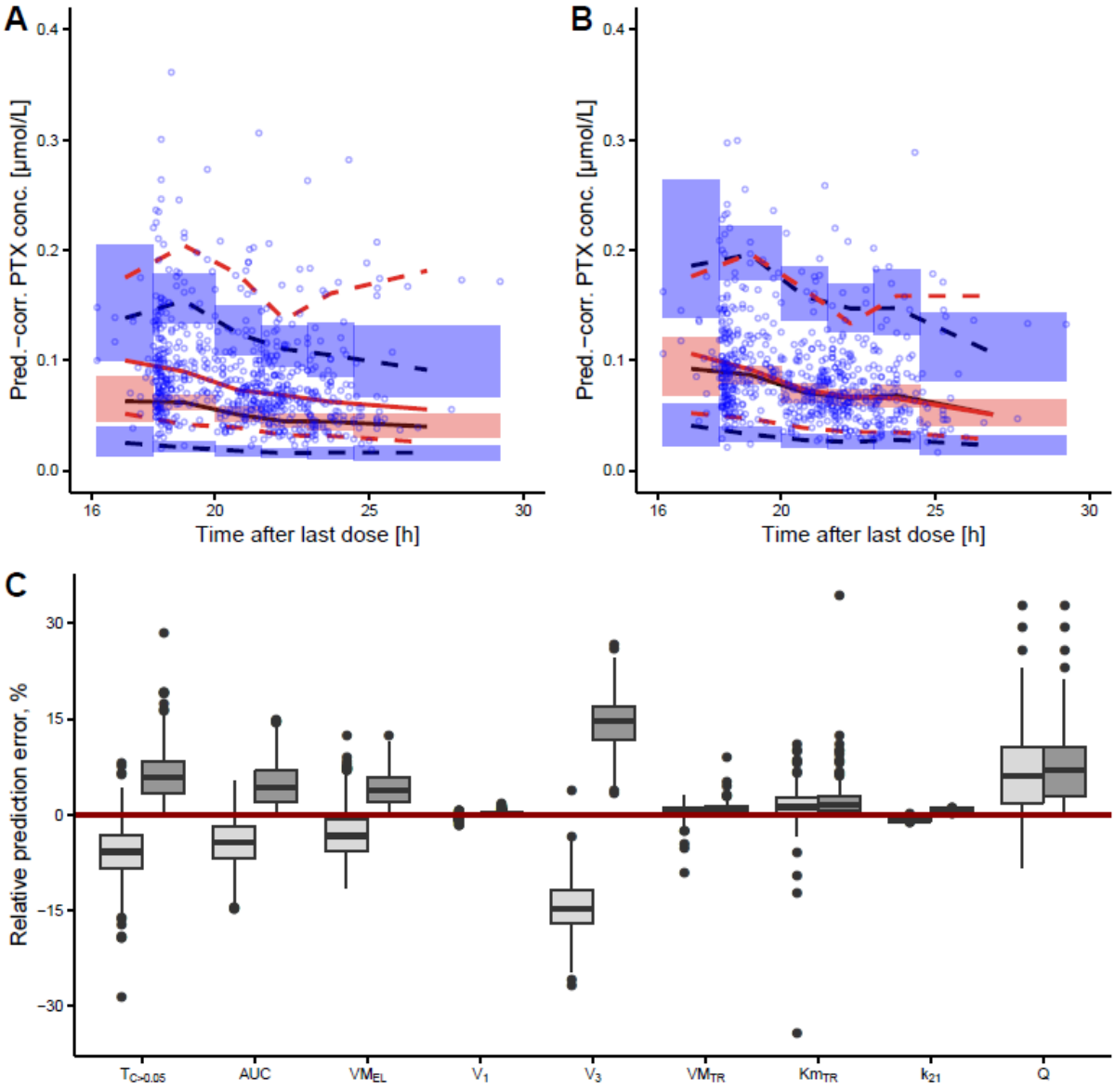

JPET Fast Forward. Published on June 9, 2017 as DOI: 10.1124/jpet.117.240309
This article has not been copyedited and formatted. The final version may differ from this version.

Fig. 3

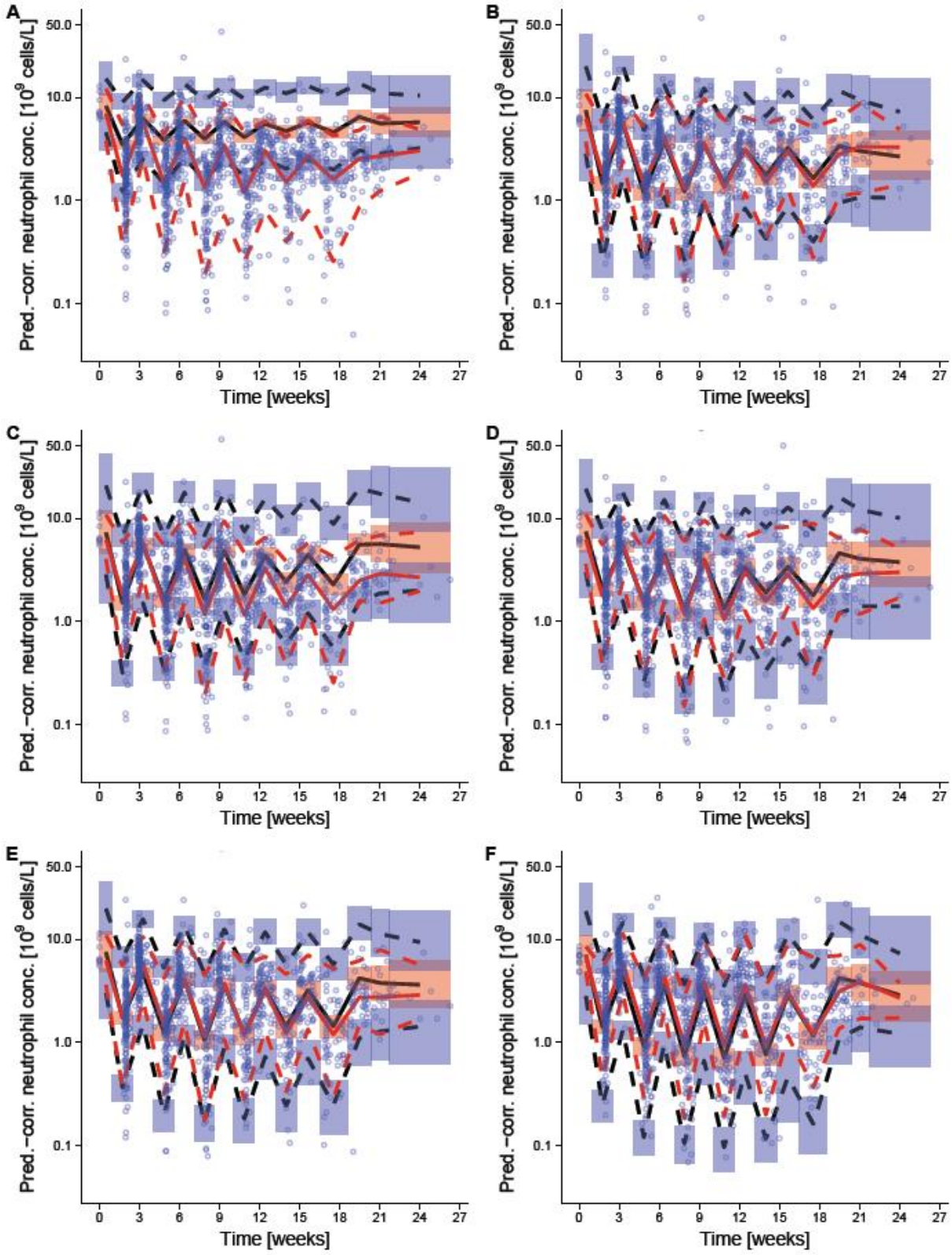

JPET Fast Forward. Published on June 9, 2017 as DOI: 10.1124/jpet.117.240309
This article has not been copyedited and formatted. The final version may differ from this version.

Fig. 4